THE JOURNAL OF BIOLOGICAL CHEMISTRY
Vol. 279, No. 11, Issue of March 12, pp. 10222–10227, 2004

Printed in U.S.A.

Serpin Mechanism of Hepatitis C Virus Nonstructural 3 (NS3) Protease Inhibition

INDUCED FIT AS A MECHANISM FOR NARROW SPECIFICITY*

Received for publication, December 18, 2003
Published, JBC Papers in Press, December 29, 2003, DOI 10.1074/jbc.M313852200

Martin J. Richer‡, Luiz Juliano§, Carl Hashimoto¶, and François Jean‡‖

From the ‡Department of Microbiology and Immunology, The University of British Columbia, Vancouver, British Columbia V6T 1Z3, Canada, the §Department of Biophysics, Escola Paulista de Medicina, Sao Paulo SP 04044-020, Brazil, and the ¶Department of Cell Biology, Yale University School of Medicine, New Haven, Connecticut 06520

Hepatitis C virus (HCV) nonstructural 3 (NS3) serine protease disrupts important cellular antiviral signaling pathways and plays a pivotal role in the proteolytic maturation of the HCV polyprotein precursor. This recent discovery has fostered the search for NS3 protease inhibitors. However, the enzyme's unusual induced fit behavior and peculiar molecular architecture have imposed considerable obstacles to the development of small molecule inhibitors. In this article, we demonstrate that such unique induced fit behavior and the chymotrypsin-like catalytic domain can provide the structural plasticity necessary to generate protein-based inhibitors of the NS3 protease. We took advantage of the macromolecular scaffold of a *Drosophila* serpin, SP6, which intrinsically supports chymotrypsin-like enzyme inhibition, to design a novel class of potent and selective inhibitors. We show that altering the SP6 reactive site loop (RSL) resulted in the development of the first effective (K_i of 34 nM) and selective serpin, $SP6^{EVC/S}$, directed at the NS3 protease. $SP6^{EVC/S}$ operates as a suicide substrate inhibitor, and its partitioning between the complex-forming and proteolytic pathways for the NS3 protease is HCV NS4A cofactor-dependent and -specific. Once bound to the protease active site, $SP6^{EVC/S}$ partitions with equal probability to undergo proteolysis by NS3 at the C-terminal site of the engineered RSL, (P_6)Glu-Ile-(P_4)Val-Met-Thr-(P_1)Cys-↓-(P_1')Ser, or to form a covalent acyl-enzyme complex characteristic of cognate protease-serpin pairs. Our results also reveal a novel cofactor-induced serpin mechanism of enzyme inhibition that could be explored for developing effective and selective inhibitors of other important induced fit viral proteases of the *Flaviviridae* family such as the West Nile virus NS3 endoprotease.

Hepatitis C virus (HCV)[1] infection has reached worldwide epidemic proportions, with >3% of the world population infected and 3–4 million people newly infected each year (1). The clinical significance of HCV and the need to rapidly identify new therapeutic approaches has resulted in intensive study of the molecular properties of this virus; yet, thus far, no efficient therapy or vaccine exists (1, 2). Moreover, although considerable progress has been made in understanding HCV biology (3, 4), the molecular mechanisms by which HCV induces liver cirrhosis, fibrosis, and hepatocellular carcinoma remain unclear (1). The discovery that HCV nonstructural 3 (NS3) protease may be involved in the modulation of important host cell functions (5), in addition to its role in the maturation of the viral polyprotein precursor (NS3-NS5) (6), has fostered the search for NS3 protease inhibitors (2, 7).

The NS3 protease is an induced fit serine protease that adopts a chymotrypsin-like fold (8). The action of a virus-encoded protein cofactor, NS4A, is required for some but not all of the NS3-dependent proteolytic cleavage events *in vitro* (9) and *ex vivo* (10, 11). The commonly accepted model of action for the NS3 protease suggests that the protease undergoes an induced fit in the presence of the NS4A cofactor (12, 13) and substrate/inhibitor (14). Intercalation of NS4A into the N-terminal domain of NS3 results in a rearrangement of the active site, consistent with the observed increase in the catalytic efficiency reported for the recombinant NS3/4A protease (15, 16).

The proposed mechanism of substrate-induced protease activation provides a framework to explain how the NS3 protease could be partially active even in the absence of the NS4A cofactor (15, 16). Unlike proteases of the long chain subfamily (17), such as human elastase, NS3 protease has short loops resulting in a featureless, shallow, and solvent-exposed substrate binding site, a feature that makes development of small molecule inhibitors difficult (2, 7). The interaction between the NS3 protease and its substrates is characterized by a series of weak contacts that extend over 10 amino acid residues, requires a cysteine in the P_1 position, and relies on high charge densities (17). Thus, substrate recognition by the NS3 protease is more reminiscent of the protein-protein interactions found in an enzyme-protein inhibitor pair than of a "conventional" enzyme-substrate complex (12, 17).

In this article, we hypothesized that the bioengineering of a naturally occurring serine protease inhibitor (serpin) scaffold could provide a new approach to developing high affinity, selective NS3 protease inhibitors (18, 19). Serpins differ from

* This study was supported by a Canadian Institutes of Health Research/Health Canada Research Initiative on Hepatitis C Scholarship and Grant EOP38153 (to F. J.), National Institutes of Health Grant GM49370 (to C. H.), and by Fundação de Amparo à Pesquisa do Estado de São Paulo (FAPESP), Conselho Nacional de Desenvolvimento Cientifico e Technologico (CNPq), and Human Frontiers for Science Progress Grant RG-00043/2000-M) (to L. J.). The costs of publication of this article were defrayed in part by the payment of page charges. This article must therefore be hereby marked "*advertisement*" in accordance with 18 U.S.C. Section 1734 solely to indicate this fact.

‖ To whom correspondence should be addressed: Dept. of Microbiology and Immunology, The University of British Columbia, 300-6174 University Blvd., Vancouver, British Columbia V6T 1Z3, Canada. Tel.: 604-822-0256; Fax: 604-822-6041; E-mail: fjean@interchange.ubc.ca.

[1] The abbreviations used are: HCV, hepatitis C virus; NS, nonstructural; RSL, reactive site loop; RP-HPLC, reverse phase high pressure liquid chromatography; MALDI-TOF, matrix-assisted laser desorption/ionization time-of-flight; MS, mass spectrometry; IQFS, intramolecularly quenched fluorogenic substrate; SI, stoichiometry of inhibition; Abz, *ortho*-aminobenzoic acid: EI*, enzyme-inhibitor complex; GBV, GB virus (A, B, or C).

non-serpin inhibitors in that they require a large inhibitor conformational change in order to trap proteases in an irreversible complex (20). The conformational change is initiated by the reaction of the active serine of the protease with the reactive site loop (RSL) of the serpin that results in a covalent species involving an acyl ester linkage to the γO of the protease active site serine. This cleaves the RSL, which then moves 71 Å to the opposite pole of the serpin, taking the tethered protease with it (20, 21).

We selected a *Drosophila* serpin, SP6, to serve as a prototype of the macromolecular inhibitor scaffold, because SP6 has been shown to inhibit chymotrypsin-like proteases (22). We show that engineering of the RSL of SP6 resulted in the development of $SP6^{EVC/S}$, the first selective and effective serpin directed at the NS3 protease. $SP6^{EVC/S}$ operates as a suicide substrate inhibitor with the slow tight binding mechanism characteristic of serpin molecules. Partitioning between the covalent serpin acyl-enzyme complex-forming and proteolytic pathways for NS3 protease is both HCV NS4A cofactor- and serpin-dependent, supporting the recent model of cofactor- and substrate-induced NS3 activation as a mechanism of narrow specificity (23).

EXPERIMENTAL PROCEDURES

Materials—pyroGlu-Arg-Thr-Lys-Arg-4-methylcoumaryl-7-amide (pERTKR-MCA) was obtained from Bachem, trypsin (EC: 3.4.21.4) from Sigma, and anti-FLAG from Affinity Bioreagents.

Synthesis of Peptidyl Analogs—All peptides were prepared by solid phase synthesis with the Fmoc (*N*-(9-fluorenyl)methoxycarbonyl) methodology using a multiple automated peptide synthesizer (24). Peptide purity and composition was demonstrated by reverse phase HPLC (RP-HPLC), matrix-assisted laser desorption ionization time-of-flight (MALDI-TOF) mass spectrometry (MS), and amino acid analysis (University of Toronto Advanced Protein Technology Center). The following peptides were used in this study: Ac-KKKGSVVIVGRIILSGR-NH_2 (HCV-Pep4A); Ac-KKKGSVVVVGRIILSGR-NH_2 (HCV-I25V); Ac-KKKGSVVIVGRWILSGR-NH_2 (HCV-I29W); Ac-KKKGSVVVVGRWILSGR-NH_2 (HCV-I25V/I29W); Ac-KKKGSLVVVTSWVVNGN-NH_2 (GBVA-Pep4A); Ac-KKKGATCVRRCWSITSV-NH_2 (GBVB-Pep4A); and Ac-KKKGSLVVVTDWDVKGG-NH_2 (GBVC-Pep4A). Full details of the synthesis and biochemical characterization of Abz-Asp-Asp-Ile-Val-Pro-Cys-Ser-Met-Ser-Tyr(NO_2)-Thr-NH_2 (IQFS-1) and (fluorescein)-Asp-D-Glu-Leu-Ile-Cha-Cys-Pro-Cha-Asp-Leu-NH_2 (PepInh-1) (where Cha is cyclohexylalanine) will be presented elsewhere. Stock peptide solutions (10 mM) were prepared in Me_2SO and stored at −20 °C.

The His-tagged HCV NS3 Serine Protease and His/FLAG-tagged SP6 Variants—His-tagged NS3 expression plasmid encoding the N-terminal 181 amino acids of NS3 was kindly provided by Dr. N Kakiuchi, National Institute of Bioscience and Human Technology of Japan (25). His/FLAG-tagged SP6 was prepared from pET21a-SP6 (22) by standard PCR methods using an oligonucleotide primer encoding the FLAG epitope (Fig. 1). Desired changes in the RSL of parental SP6 were introduced using the QuikChange site-directed mutagenesis method (Stratagene). Primers incorporating the desired changes were synthesized by Alpha DNA Inc. Multiple amino acid changes were introduced by sequential rounds of mutagenesis using newly synthesized SP6 variants as template. Introduction of the desired changes was confirmed by sequencing (Sheldon Biotechnology Center, McGill University, Montreal, Canada).

Expression and Purification of HCV NS3 and Recombinant SP6 Variants—Recombinant NS3 protease and SP6 variants were expressed in the cytosol of bacteria (*Escherichia coli* BL21 pLysS) and purified as reported previously (18) by nickel binding interaction chromatography (HiTrap Columns; Amersham Biosciences) using an AKTApurifier FPLC system (Amersham Biosciences). Protein purity and composition were demonstrated by RP-HPLC (18), MALDI-TOF MS (Fig. 1) (University of Victoria-Genome British Columbia Proteomics Facility), Western blot (Fig. 2), and amino acid analysis (University of Toronto). Proteins were aliquoted, snap frozen, and stored at −86 °C.

Enzymatic Assays—The enzyme assay data were obtained by using a SpectraMax Gemini XS spectrofluorometer equipped with a temperature-controlled 96-well plate reader (Molecular Dynamics) using excitation/emission wavelengths of 370/460 nm to measure release of 7-amido-4-methylcoumarin (AMC) (16) or 320/420 nm to measure the fluorescence signal of Abz-DDIVPC-OH (26). Trypsin assays were performed using pyroGlu-Arg-Thr-Lys-Arg-4-methylcoumaryl-7-amide as a fluorogenic substrate (27), whereas a novel intramolecularly quenched fluorogenic peptide substrate (IQFS-1), based on the fluorescence energy transfer between the donor/acceptor couple (Abz and Tyr(NO_2)), was used for NS3 protease (26). Trypsin assays were performed at 30 °C in 100 mM Hepes (pH 7.3) containing 1 mM $CaCl_2$ and 0.5% Triton X-100. NS3 protease assays were performed at 30 °C in 50 mM Hepes (pH 7.3), 1 mM dithiothreitol, 100 mM NaCl, and 0.1% Triton X-100. An NS3/4A protease heterocomplex was generated by preincubating NS3 with a saturating amount of HCV-Pep4A (7 μM) for 15 min at 30 °C (16).

SDS-PAGE of Protease-Serpin Reactions—Reactions were performed under the buffer conditions for enzyme assays. Samples were collected at 1 h (unless otherwise noted), mixed immediately with reduced SDS-loading buffer at 95 °C, and heated for 10 min. SDS-gel electrophoresis (18) was performed in a 10% gel, and the protein was visualized by Coomassie Blue or analyzed by Western blotting using anti-FLAG antibody following transfer to nitrocellulose (18, 19). Western blots were visualized directly using the VersaDoc imaging system (Bio-Rad). The resulting digital images were quantified using Quantity One software (Bio-Rad).

Determination of the RSL Cleavage Site and Covalent Serpin-Protease Complex Formation by MS—$SP6^{C/S}$ and $SP6^{EVC/S}$ (0.2 μM) were incubated with NS3/4A (2 μM:7 μM) for 1 h at 30 °C. Reactions were stopped with an aqueous 0.3% (v/v) CF_3COOH solution (final 0.1% (v/v) CF_3COOH). Stoichiometry ($[I_0]$ /$[E_0]$) was chosen so that the reaction products were generated at sufficient levels to be detected by MALDI-TOF MS (University of Victoria). Alternatively, after completion, products were resolved on a 10% SDS gel. The high molecular weight complex band (EI*) was visualized with Coomassie Blue and excised from the gel. Trypsin digestion of the protein was performed by in-gel cleavage (28). The resulting peptide fragments were recovered by a series of extractions using 10% formic acid, and the mixture was resolved by RP-HPLC. Identification of each peptidyl fragment was performed using a quadruple TOF MS (University of Victoria).

Stoichiometry of Inhibition (SI) and Determination of K_i—Values for SI and K_i were determined as described previously (18) using active-site titrated NS3/4A protease. The active concentration of NS3/4A protease was determined by active site titration with PepInh-1, a novel tight-binding reversible inhibitor of NS3/4A protease (K_i = 2.8 ± 0.2 nM).[2] Subsequent titrations were performed by pre-incubating each serpin variant with NS3 or NS3/4A for 30 min at 30 °C and adding increasing amounts of inhibitors to a fixed amount of protease. The residual protease activity was determined by the addition of IQFS-1 (100 μM). $[E_0]$ and K_i were obtained as described previously (18, 29). Measurements were also made using the progress curve method for the reaction started with enzyme (18).

RESULTS

Engineering Drosophila SP6 Scaffold to Target the HCV NS3 Viral Protease—Because previous studies have demonstrated that SP6 architecture can inhibit chymotrypsin-like serine proteases (22), we selected this novel *Drosophila* serpin scaffold to bioengineer an inhibitor directed at the NS3 protease. The design of the SP6-RSL was based on a quantitative kinetic analysis performed with IQFSs based on NS3-dependent cleavage sites of the HCV polyprotein.[3] We observed that the binding energy for the substrate is derived from a series of weak interactions distributed along an extended contact surface (P_6–P_4') (30). The major determinants of substrate recognition include conserved residues in (P_1)Cys, (P_1')Ser, and (P_6)Glu positions. P_3, P_4 and P_4' residues also contribute to efficient substrate recognition, although less dramatically. The RSL sequence of SP6 variants prepared in this study is shown in Fig. 1 and includes single or multiple mutations introduced to optimize the interactions between the RSL of SP6 and the substrate binding sites of NS3 (S_6–S_1') (30).

Selective Inactivation of HCV NS3/4A Protease Activity by Bioengineered $SP6^{EVC/S}$—We screened for serpin inhibitory activity by incubating the SP6 variants with trypsin or NS3/4A

[2] M. J. Richer, P. Hamill, and F. Jean, unpublished results.

[3] M. J. Richer, M. M. Martin, A. Po, L. Juliano, and F. Jean, unpublished results.

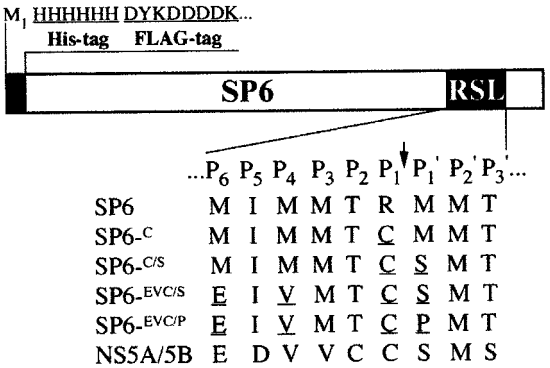

FIG. 1. **SP6 variants and amino acid sequences of the engineered RSL.** The positions and substitutions within the RSL of each variant are shown. Engineered residues are *underlined* and correspond to the NS5A/5B NS3 cleavage site of the HCV polyprotein. The measured molecular mass of each variant was determined by MALDI-MS and was in close agreement (relative error <0.08% for the following: SP6, 43,978.33; $SP6^{C}$, 43,948.06; $SP6^{C/S}$, 43,877.07; $SP6^{EVC/S}$, 43,819.95; and $SP6^{EVC/P}$, 43,857.70) with the corresponding calculated value.

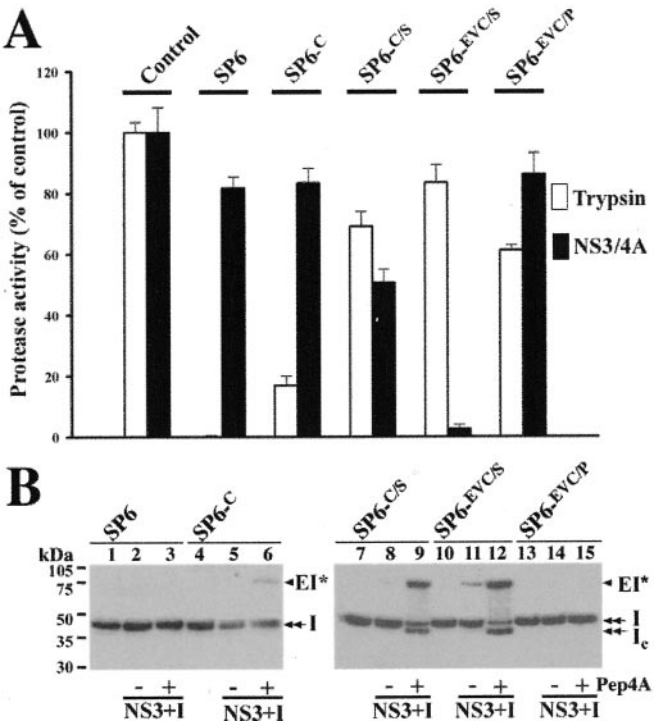

FIG. 2. **Inhibition of HCV NS3/4A protease by SP6 variants.** *A*, survey of SP6 variant inhibition against trypsin (*open bars*) or NS3/4A (*filled bars*). Trypsin (76.5 pM) or NS3/4A complex (98.5 nM:7 μM) was incubated with each SP6 variant (0.5 μM), and residual proteolytic activity was measured. The data are averages of duplicate samples and are representative of three independent experiments. *B*, SDS-PAGE analysis of reactions of NS3 (2.0 μM) or NS3/4A (2 μM:7 μM) with SP6 variants (0.2 μM). Samples were processed for Western blot analysis, and FLAG-tagged proteins were detected using a polyclonal FLAG-tag antibody. Shown is one of the three independent experiments. The locations of the inhibitor (I), cleaved inhibitor (I_c), and enzyme-inhibitor complexes (EI*) are indicated.

before adding the appropriate substrate (Fig. 2*A*). Although the native SP6 inhibited trypsin completely, it was not effective against NS3/4A protease activity (Fig. 2*A*). As predicted, engineering the SP6-RSL to include all the key molecular determinants needed for optimum recognition by the viral protease generates a serpin ($SP6^{EVC/S}$) that efficiently inactivates NS3/4A protease activity (Fig. 2*A*). Importantly, optimizing the RSL of SP6 to target NS3 also resulted in a loss of trypsin inhibition. $SP6^{C/S}$, whose RSL is lacking the P_4 and P_6 mutations, inhibited both trypsin and NS3. The inhibition of trypsin was less efficient and did not involve a classical serpin mechanism (no apparent SDS-heat stable complex; data not shown). Substitution of the serine residue in P_1' position of $SP6^{EVC/S}$ by a proline residue ($SP6^{EVC/P}$) resulted in a loss of inhibitory activity against NS3/4A protease (Fig. 2*A*). This was a surprising result, because a similar substitution in a synthetic peptidyl substrate based on the HCV NS5A/5B junction resulted in a competitive inhibitor of NS3 (31). This first survey of inhibitory activity of the SP6 variants confirmed the potential of SP6 as a scaffold to design NS3 specific inhibitors.

HCV-Pep4A Is Required for Specific Interaction of HCV NS3 Protease with Serpin—The influence of the HCV-Pep4A (NS4A cofactor, residues 21–34; Fig. 5) on the mechanism of inhibition of NS3 protease by the SP6 variants was evaluated. SP6 variants were incubated with NS3 or NS3/4A, and the reactions were analyzed by Western blot (Fig. 2*B*). Incubation of each serpin in the absence of NS3 protease showed a single ~44-kDa protein (Fig. 2*B*, *lanes 1*, *4*, *7*, *10*, and *13*), which corresponds to the predicted mass of the SP6 variants (Fig. 1). Including HCV-Pep4A in the incubation with NS3 resulted in a shift of $SP6^{C/S}$ and $SP6^{EVC/S}$ (Fig. 2*B*, *lanes 6*, *9*, and *12*) to a single high M_r band (~70 kDa) corresponding to the predicted molecular masses of serpin-NS3 complexes (64.4 kDa). Native SP6, $SP6^{C}$, and $SP6^{EVC/P}$ could not form a complex with NS3/4A (less than 2% with $SP6^{C}$), and the SP6 variants were not cleaved, indicating that these variants are not effective inhibitors of NS3 (Fig. 2B, *lanes 3*, *6*, and *15*). In contrast, the EI* complex observed with $SP6^{C/S}$ and $SP6^{EVC/S}$ was associated with the presence of the cleaved forms (I_c ~ 39 kDa) of the serpin (Fig. 2*B*, *lanes 9*, 12). These data indicate that $SP6^{C/S}$ and $SP6^{EVC/S}$, in the presence of HCV-Pep4A, can interact with the protease. We concluded that HCV-Pep4A is required for efficient formation of SDS-stable complexes between NS3 protease and $SP6^{C/S}$ or $SP6^{EVC/S}$.

HCV NS3 Protease Forms a Stable Covalent Acyl-Enzyme Complex with $SP6^{EVC/S}$—MS analysis was used to identify the high M_r band resolved on SDS-PAGE for the NS3/4A-$SP6^{EVC/S}$ reaction (Fig. 2*B*, *lane 12*). MS/MS sequence analysis of five tryptic peptidyl fragments from the high M_r band was obtained. Four of the fragments sequenced were derived from SP6 (^{15}FTSELFQLLSAGGLK^{29}, ^{146}ITELVSADSFSDNTR^{160}, ^{161}LVLLNALHFK^{170}, and ^{239}TGIYALAEK^{247}), and one corresponded to the NS3 protease (^{12}GLLGCIITSLTGR^{24}). These results are consistent with the idea that the high M_r band detected by Western blot is an SDS-heat stable serpin acyl-enzyme complex.

MALDI-MS was used to demonstrate the formation of a covalent serpin acyl-enzyme complex between $SP6^{EVC/S}$ and NS3 protease. MS analysis of the NS3/4A-$SP6^{EVC/S}$ reaction performed in optimized conditions to yield maximum amounts of complexes revealed the presence of stable covalent species with an observed mass of 64308.88 (Fig. 3*B*). The calculated mass for the NS3-$SP6^{EVC/S}$ serpin-protease complex is 64427.41 (relative error 0.18%). Other species detected included the liberated $SP6^{EVC/S}$ N-terminal (39845.62) (Fig. 3*B*) and C-terminal (3932.05) (Fig. 3*A*) fragments, native NS3 protease (24338.00) (Fig. 3*B*), and HCV-Pep4A (1851.31) (Fig. 3*A*). Thus, MS analysis of the NS3/4A-$SP6^{EVC/S}$ reaction revealed products consistent with the formation of a covalent complex (inhibitor pathway) characteristic of serpin-enzyme interactions and cleavage of the engineered RSL at the P_1 position (substrate pathway) (20).

$SP6^{EVC/S}$ Inhibits HCV NS3/4A Protease by the Slow Tight Binding Mechanism Characteristic of Serpin Molecules—The

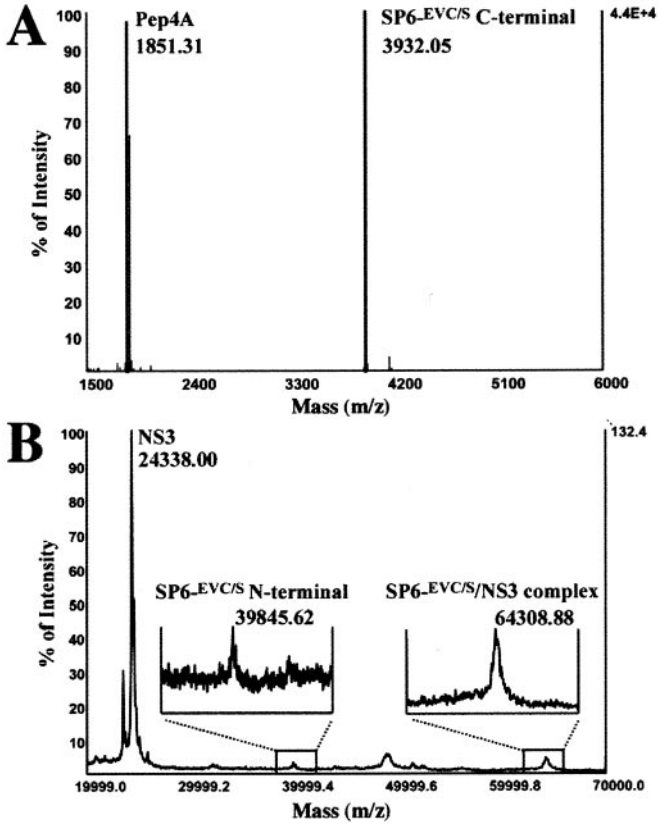

FIG. 3. **MALDI-MS analysis of NS3/4A-SP6$^{EVC/S}$ reactions.** NS3/4A (2.0 μM: 7.0 μM) was incubated with SP6$^{EVC/S}$ (0.2 μM). Reactions were stopped and analyzed by MALDI-MS. Shown are the experimental mass values for the SP6$^{EVC/S}$ C-terminal product (*A*), the SP6$^{EVC/S}$ N-terminal fragment (*B*, *left*), and the covalent acyl-enzyme NS3-SP6$^{EVC/S}$ complex (*B*, *right*). The molecular masses observed for the liberated C-terminal fragment, N-terminal fragment, and serpin acyl-enzyme complex were in good agreement (relative error, $< 0.08\%$) with the calculated molecular mass values. Pep4A and NS3 were also resolved and are shown in *panels A* and *B*, respectively.

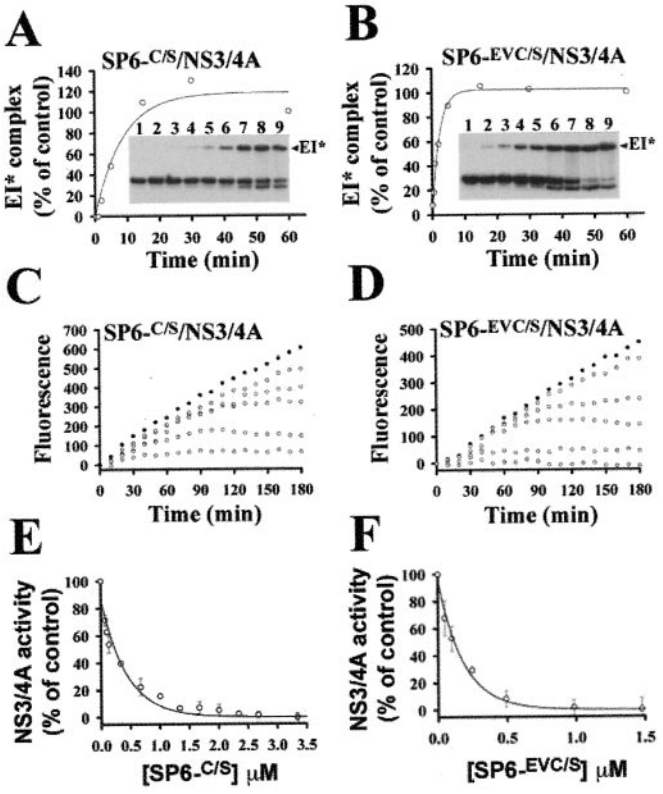

FIG. 4. **Mechanism of NS3/4A inhibition by SP6$^{C/S}$ and SP6$^{EVC/S}$.** The time course of complex formation between SP6$^{C/S}$ (*A*) and SP6$^{EVC/S}$ (*B*) with NS3/4A is shown. SP6 variants (0.2 μM) and NS3/4A (2 μM:7 μM) were incubated, and the reactions were stopped and processed for Western blot at each time point (*inset*). The density of the complex bands (EI*) was determined using the VersaDoc system and then analyzed with Enzfitter software to determine the rate of complex formation. The *lanes* correspond to 0, 10, 30, 60, 120 s and 5, 15, 30, and 60 min. Shown is one of three independent experiments. Slow binding inhibition kinetics of NS3/4A protease by SP6$^{C/S}$ (*C*) and SP6$^{EVC/S}$ (*D*) are shown. NS3/4A (1 μM:7 μM) was incubated with IQFS-1 (50 μM) in the absence (*closed circle*) or presence of SP6 variants (SP6$^{C/S}$, 0.6 (*top*) and 1.4, 2.8, 5.7, or 7.1 μM (*bottom*); SP6$^{EVC/S}$, 19.7 (*top*) and 59.1, 98.4, 196.9, or 393.8 nM (*bottom*)). Data are representative of the three independent experiments. Tight binding titration of NS3/4A by SP6$^{C/S}$ (*E*) and SP6$^{EVC/S}$ (*F*) are shown. NS3/4A (2 μM:7 μM) was incubated with increasing amounts of SP6 variants for 30 min. IQFS-1 (50 μM) was added to determine residual NS3/4A activity. For each serpin, the calculated ratio of $[E_0]/K_i$ was superior to 2, validating the values obtained for SP6$^{C/S}$ and SP6$^{EVC/S}$ as tight-binding titrants of NS3/4A (18, 29). The data are averages of duplicate samples and are representative of three independent experiments.

temporal relationship between complex formation and inhibition of NS3 protease activity was examined. The rate of complex formation (k_{obs}) of NS3/4A protease by SP6$^{C/S}$ and SP6$^{EVC/S}$ was examined by SDS-PAGE, and the value was determined as described previously (32) (Fig. 4). NS3 or NS3/4A was combined with each of the serpin variants, and complex formation was measured at various time points (Fig. 4, *A* and *B*). The k_{obs} with NS3/4A protease for SP6$^{EVC/S}$ ($3.3 \pm 0.4 \times 10^{-2}$ s^{-1}) is ~3× more rapid than the value estimated for SP6$^{C/S}$ ($1.2 \pm 0.2 \times 10^{-2}$ s^{-1}). In the absence of HCV-Pep4A, the rate of serpin-protease complex formation was much slower (SP6$^{EVC/S}$-NS3, 50% complete ($t_{1/2}$) at 4 h; SP6$^{C/S}$-NS3 $< 1\%$ at 4 h; data not shown). By comparison, the $t_{1/2}$ values of SP6$^{EVC/S}$-NS3/4A and SP6 trypsin complex formation were 85 s (Fig. 4*B*) and 20 s (data not shown), respectively. Typical of serpin-enzyme interactions, the inhibition of NS3/4A by SP6$^{C/S}$ (Fig. 4*C*) and SP6$^{EVC/S}$ (Fig. 4*D*) obeyed slow binding inhibition kinetics as indicated by biphasic plots in which maximal inhibition was achieved more rapidly with increasing concentrations of serpin (18). The serpin-enzyme complexes were kinetically trapped, because no NS3 protease activity was recovered for up to 3 h (Fig. 4, *C* and *D*). These results confirm the SDS-PAGE analysis (Fig. 4, *A* and *B, insets*) and support the formation of covalent complexes demonstrated by MS analyses (Fig. 3*B*).

SP6$^{EVC/S}$ Is a Tight Binding Titrant of the HCV NS3/4A Protease—After formation of the serpin/enzyme acyl intermediate (EI′) (20), serpins may either be cleaved and released (I_c) or trap the enzyme in a kinetically stable SDS-resistant complex (EI*) (Fig. 4*B*, *inset*) (20). The relative flux of a serpin through these pathways reflects its efficiency as an inhibitor for a given enzyme and is described as the stoichiometry of inhibition (20). SI is defined as the ratio of moles of serpin needed to inhibit 1 mol of protease (20). Titration experiments were performed to determine the SI for NS3/4A-SP6$^{C/S}$ and NS3/4A-SP6$^{EVC/S}$ (18, 29). The concentration of NS3/4A ($[E_0]$) was determined by titrating the enzyme activity with PepInh-1 (data not shown). In a parallel analysis, NS3/4A activity was titrated with SP6$^{C/S}$ (Fig. 4*E*) or SP6$^{EVC/S}$ (Fig. 4*F*). Regression analysis of residual NS3/4A activity as a function of $[I_0]/[E_0]$ shows that SP6$^{C/S}$ inhibits NS3 with an SI of ~4 (3.8), whereas SP6$^{EVC/S}$ inhibits with an SI of ~2 (2.1). This means that, after binding to the active site of NS3, SP6$^{EVC/S}$ partitions with equal probability between the substrate and the inhibition pathways (20). Analysis of the titrations by curve fitting (Fig. 4, *E* and *F*) revealed an overall K_i of 125 ± 16 nM for NS3/4A-

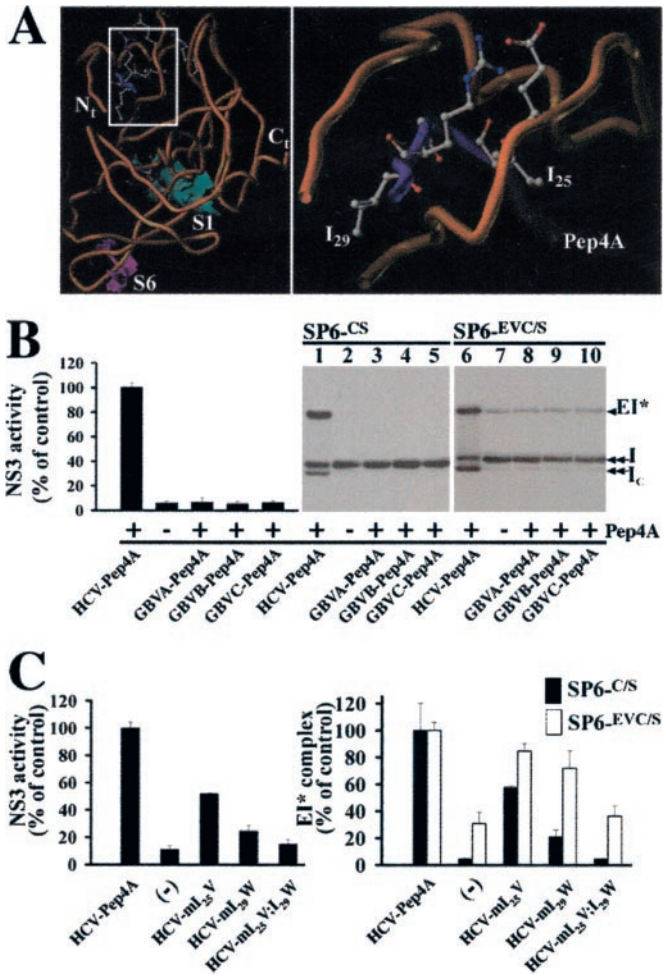

FIG. 5. **Mechanistic role of the NS4A peptide cofactor in the ternary enzyme-activator-serpin complex.** *A*, molecular architecture of the NS3/Pep4A heterocomplex. *Left panel*, ribbon representation of HCV NS3 (residues 1–189; *yellow*) complexed with HCV-Pep4A (residues 21–34; *purple*). Structure was compiled by using the SYBYL version 6.6 software (Tripos, St Louis). *Right panel*, closer representation of the central region of NS4A (Pep4A) that tightly intercalates within a β-sheet of the enzyme core via hydrophobic interactions. Residues of interest within Pep4A are *highlighted*. *B*, stimulatory effects of other NS4A functional homologues from the *Flaviviridae.* NS3 protease was preincubated with saturating amounts of peptide cofactors (7.0 μM). NS3 protease (98.5 nM) activity (*left panel*) and protease-serpin complex formation (*center* and *right panels*) were determined as described (see "Experimental Procedures") (NS3-SP6, 2 μM:0.2 μM). *C*, role of Ile^{25} and Ile^{29} of the NS4A on serpin acyl-enzyme complex formation. The effect of HCV-Pep4A variants (7 μM) on NS3 protease activity and complex formation with SP6 variants were analyzed as described above. The data are averages of duplicate samples and are representative of three independent experiments.

$SP6^{C/S}$ and 34 ± 5 nM for NS3/4A-$SP6^{EVC/S}$. These results indicated that $SP6^{EVC/S}$ is a tight binding titrant of the NS3/4A protease operating as a suicide substrate inhibitor.

HCV NS4A Is an Obligate Cofactor for HCV NS3 Protease Inhibition by $SP6^{EVC/S}$—We evaluated the stimulatory effects of other NS4A functional homologues from the *Flaviviridae* family (33). We synthesized three NS4A peptides containing the putative minimal activating NS4A sequence (amino acids 22–33) of GBVA, GBVB, and GBVC (34). Analysis of the products of the NS3/4A/serpin reactions showed that only HCV-Pep4A significantly enhanced complex formation (Fig. 5*B*, *lanes 1* and *6*). As a control, we measured the stimulatory effects of the NS4A peptides in trans-cleavage reactions using IQFS-1. The results showed that cleavage strictly depends on the addition of HCV-Pep4A (Fig. 5*B*, *left panel*). No other NS4A analog could activate NS3 protease activity even when used in 5-fold excess of the saturating concentration for HCV-Pep4A (data not shown). Thus, the cofactor dependence for complex formation parallels the changes seen for enzymatic activity, for which only the presence of HCV-Pep4A increases hydrolysis rates.

Role of Ile^{25} and Ile^{29} of the NS4A on Serpin Acyl-Enzyme Complex Formation—Comparison of the primary sequences of *Flavivirus* NS4A functional homologues with several *Hepacivirus* strains demonstrates that hydrophobic amino acids are highly conserved at positions 25 and 29 of the central region of NS4A protein (data not shown). Although these two residues are strictly conserved within isolates of the same genus, they differ markedly across the *Hepacivirus* and *Flavivirus* strains (Fig. 5*A*). We synthesized three HCV-Pep4A variants by substituting residues at positions 25 (HCV-I25V), 29 (HCV-I29W), and 25 and 29 (HCV-I25V/I29W) for the corresponding residues conserved in NS4A of GBVs. Analysis of the products of the NS3/4A/serpin reactions showed that mutation at Ile^{25} or Ile^{29} had an important effect on $SP6^{C/S}$-NS3 complex formation with cofactor activity values reduced to ~56.5% (HCV-I25V) and 20.3% (HCV-I29W) of wild-type levels (Fig. 5*C*, *right panel*). The double mutations at Ile^{25} and Ile^{29} (HCV-I25V/I29W) had a more dramatic effect, reducing activity to only 3.6% of wild-type. In contrast, the effect of the individual mutations (Ile^{25} or Ile^{29}) was less pronounced with the $SP6^{EVC/S}$ variant (87.1% and 69.7%), with complete reduction of the NS4A-mediated complex activation observed only when the reaction was performed with the double mutant, HCV-I25V/I29W (Fig. 5*C*, *right panel*). It should be noted that $SP6^{EVC/S}$ can form an acyl-enzyme complex via an NS4A-independent mechanism (30.6% of wild-type control), supporting a plausible role for the serpin itself in enzyme activation (Fig. 5*C*, *right panel*).

The effects that these substitutions in the HCV-Pep4A impart on the active site of NS3 protease were investigated using IQFS-1 (Fig. 5*C*, *left panel*). We found that substituting residues 25 and 29 individually with the corresponding residues from GBV NS4A resulted in a substantial decrease in the NS3/4A endoproteolytic activity (HCV-I25V, 51.8%; HCV-I29W, 24.5%) (Fig. 5 *C*, *left panel*). The double mutant of NS4A cofactor peptide, HCV-I25V/I29W, had little cofactor activity (15.3%) (Fig. 5*C*, *left panel*). The requirement of the same functional domain and hydrophobic amino acids of NS4A for each trans-processing activity of NS3 (serpin or substrate recognition and catalysis) indicated a critical role for NS4A in these two biochemical pathways and a complex interplay between the cofactor, viral protease, and serpin. This is further supported by the important increase in K_i (127 ± 13 nM) and SI (8.3 ± 0.6) determined for NS3/$SP6^{EVC/S}$ in the presence of HCV-I29W (data not shown). Taken together, the results of this study indicate the critical requirement of a fully activated heterodimeric protease (NS3/4A) for $SP6^{EVC/S}$ to effectively form a complex with and inhibit the NS3 protease.

DISCUSSION

This article presents the design and characterization of a novel class of potent and selective HCV NS3 protein inhibitors. We selected a novel *Drosophila* serpin, SP6, as a prototype of a protein inhibitor scaffold because it has been shown to inhibit chymotrypsin-like proteases (22). Engineering of the RSL of SP6 resulted in the development of $SP6^{EVC/S}$, the first selective and effective serpin directed at the NS3 protease. Kinetic studies have shown that $SP6^{EVC/S}$ inhibits NS3 by the slow tight binding mechanism typical of serpins and operates as a suicide substrate inhibitor. Biochemical analysis of the serpin mechanism of NS3 protease inhibition revealed that HCV NS4A is an obligate cofactor for enzyme inhibition by $SP6^{EVC/S}$.

Although many serpins identified to date have a narrow specificity, others act as broad-based protease inhibitors (20). Modifications affecting sequences and/or size of the serpin-RSL strongly influence the type of target enzymes and/or the rate of their inactivation (20). By testing the specificity of five SP6 variants, we show the importance of an appropriate RSL sequence for developing a selective and potent inhibitor of HCV NS3 protease. In particular, we demonstrate the essential requirement of three key residues within the SP6-RSL (P_1(Cys), P_1'(Ser), and P_6(Glu)) to trigger effective formation of an irreversible serpin-NS3 protease complex. These results also suggest that bioengineering of other serpin scaffolds that intrinsically support chymotrypsin-like serine protease inhibition could result in novel prototypes of the serpin-based inhibitors of HCV NS3 protease. Indeed, our preliminary studies with engineered α_1-antitrypsin variants[4] support this hypothesis.

Because enzyme inhibition by serpins is a biochemical reaction, an associated rate of inhibition can be increased or decreased by cofactors or allosteric effectors (20). The branched nature of the serpin inhibitory pathway also ensures two possible products of the reaction between serpin and protease, namely a kinetically trapped acyl-enzyme complex and a cleaved serpin. In our study on the SP6-NS3 pair, we demonstrated that the virally encoded cofactor, NS4A, regulates not only the rate of serpin-protease complex formation (k_{obs}) and the overall inhibition constant (K_i) but also the partitioning between the complex-forming and proteolytic pathways (SI). For example, we observed a 2–3 log increase in the k_{obs} values for the SP6-NS3 pair in the presence of HCV-Pep4A.

These results agree with recent findings by Bianchi *et al.* (35) and support a mechanistic model of action for NS4A in which cofactor binding induces an NS3 structure that is already, but not entirely, pre-organized for substrate/inhibitor binding. Hence, this NS4A-mediated stabilization mechanism, which helps to pre-organize the binding site, could explain in part the rapid formation of stable acyl-enzyme complexes with the SP6 variants, but only for NS3/4A heterodimeric serine protease.

Second, our kinetics studies on NS3/4A/SP6$^{C/S}$, NS3/4A/SP6$^{EVC/S}$, and NS3/4A-I29W/SP6$^{EVC/S}$ demonstrated an important contribution of each individual component of the ternary complex (protease/cofactor/serpin) in the mechanism of inhibition and the regulation of the outcome of the serpin-branched pathway. This is consistent with the recently proposed model in which, in addition to the NS4A cofactor, the substrate/substrate-based inhibitor plays an important role in activating the NS3 protease catalytic mechanism by conformational stabilization of the catalytic triad (36). We are attempting to co-crystallize NS3/4A/SP6$^{EVC/S}$ to provide structural information on this rather unique ternary complex. In addition, we are examining the potential of this novel cofactor-induced serpin mechanism of enzyme inhibition for developing effective and selective protein inhibitors of other important induced fit viral proteases from the *Flaviviridae* family (*e.g.* West Nile virus NS3 and dengue virus NS3).

[4] A. Po and F. Jean, unpublished results.

Acknowledgments—We thank Dr. M. A. Juliano for her expert assistance during peptide synthesis and Dr. N. Kakiuchi for the ΔNS3 plasmid. We also thank Drs. G. Spiegelman and J. Kelly for constructive comments and proofreading of the manuscript.

REFERENCES

1. Tan, S. L., Pause, A., Shi, Y. & Sonenberg, N. (2002) *Nat. Rev. Drug Discov.* **1,** 867–881
2. De Francesco, R., Tomei, L., Altamura, S., Summa, V. & Migliaccio, G. (2003) *Antiviral. Res.* **58,** 1–16
3. Rosenberg, S. (2001) *J. Mol. Biol.* **313,** 451–464
4. Tellinghuisen, T. L. & Rice, C. M. (2002) *Curr. Opin. Microbiol.* **5,** 419–427
5. Foy, E., Li, K., Wang, C., Sumpter, R., Jr., Ikeda, M., Lemon, S. M. & Gale, M., Jr. (2003) *Science* **300,** 1145–1148
6. Reed, K. E. & Rice, C. M. (2000) *Curr. Top Microbiol. Immunol.* **242,** 55–84
7. Narjes, F., Koch, U. & Steinkuhler, C. (2003) *Expert Opin. Investig. Drugs* **12,** 153–163
8. De Francesco, R. & Steinkuhler, C. (2000) *Curr. Top Microbiol. Immunol.* **242,** 149–169
9. Koch, J. O., Lohmann, V., Herian, U. & Bartenschlager, R. (1996) *Virology* **221,** 54–66
10. Lin, C., Pragai, B. M., Grakoui, A., Xu, J. & Rice, C. M. (1994) *J. Virol.* **68,** 8147–8157
11. Lin, C. & Rice, C. M. (1995) *Proc. Natl. Acad. Sci. U. S. A.* **92,** 7622–7626
12. Bartenschlager, R. (1999) *J. Viral Hepat.* **6,** 165–181
13. Love, R. A., Parge, H. E., Wickersham, J. A., Hostomsky, Z., Habuka, N., Moomaw, E. W., Adachi, T., Margosiak, S., Dagostino, E. & Hostomska, Z. (1998) *Clin. Diagn. Virol.* **10,** 151–156
14. Barbato, G., Cicero, D. O., Cordier, F., Narjes, F., Gerlach, B., Sambucini, S., Grzesiek, S., Matassa, V. G., De Francesco, R. & Bazzo, R. (2000) *EMBO J.* **19,** 1195–1206
15. Landro, J. A., Raybuck, S. A., Luong, Y. P., O'Malley, E. T., Harbeson, S. L., Morgenstern, K. A., Rao, G. & Livingston, D. J. (1997) *Biochemistry* **36,** 9340–9348
16. Po, A., Martin, M., Richer, M., Juliano, M. A., Juliano, L. & Jean, F. (2001) in *Peptides: The Wave of the Future, Proceedings of the 2nd International / 17th American Peptide Symposium* (Lebel, M. & Houghten, R. A., eds) pp. 563–564, Kluwer Academic Publishers, Dordrecht, The Netherlands
17. Bianchi, E. & Pessi, A. (2002) *Biopolymers* **66,** 101–114
18. Jean, F., Stella, K., Thomas, L., Liu, G., Xiang, Y., Reason, A. J. & Thomas, G. (1998) *Proc. Natl. Acad. Sci. U. S. A.* **95,** 7293–7298
19. Jean, F., Thomas, L., Molloy, S. S., Liu, G., Jarvis, M. A., Nelson, J. A. & Thomas, G. (2000) *Proc. Natl. Acad. Sci. U. S. A.* **97,** 2864–2869
20. Gettins, P. G. (2002) *Chem. Rev.* **102,** 4751–4804
21. Stratikos, E. & Gettins, P. G. (1999) *Proc. Natl. Acad. Sci. U. S. A.* **96,** 4808–4813
22. Han, J., Zhang, H., Min, G., Kemler, D. & Hashimoto, C. (2000) *FEBS Lett.* **468,** 194–198
23. Tong, L. (2002) *Chem. Rev.* **102,** 4609–4626
24. Pimenta, D. C., Fogaca, S. E., Melo, R. L., Juliano, L. & Juliano, M. A. (2003) *Biochem. J.* **371,** 1021–1025
25. Vishnuvardhan, D., Kakiuchi, N., Urvil, P. T., Shimotohno, K., Kumar, P. K. & Nishikawa, S. (1997) *FEBS Lett.* **402,** 209–212
26. Jean, F., Basak, A., DiMaio, J., Seidah, N. G. & Lazure, C. (1995) *Biochem. J.* **307,** 689–695
27. Jean, F., Boudreault, A., Basak, A., Seidah, N. G. & Lazure, C. (1995) *J. Biol. Chem.* **270,** 19225–19231
28. Kurzchalia, T. V., Gorvel, J. P., Dupree, P., Parton, R., Kellner, R., Houthaeve, T., Gruenberg, J. & Simons, K. (1992) *J. Biol. Chem.* **267,** 18419–18423
29. Knight, C. G. (1995) *Methods Enzymol.* **248,** 85–101
30. Schechter, I. & Berger, A. (1967) *Biochem. Biophys. Res. Commun.* **27,** 157–162
31. Ingallinella, P., Bianchi, E., Ingenito, R., Koch, U., Steinkuhler, C., Altamura, S. & Pessi, A. (2000) *Biochemistry* **39,** 12898–12906
32. Zhou, A., Carrell, R. W. & Huntington, J. A. (2001) *J. Biol. Chem.* **276,** 27541–27547
33. Ryan, M. D., Monaghan, S. & Flint, M. (1998) *J. Gen. Virol.* **79,** 947–959
34. Lin, C., Thomson, J. A. & Rice, C. M. (1995) *J. Virol.* **69,** 4373–4380
35. Bianchi, E., Orru, S., Dal Piaz, F., Ingenito, R., Casbarra, A., Biasiol, G., Koch, U., Pucci, P. & Pessi, A. (1999) *Biochemistry* **38,** 13844–13852
36. Barbato, G., Cicero, D. O., Nardi, M. C., Steinkuhler, C., Cortese, R., De Francesco, R. & Bazzo, R. (1999) *J. Mol. Biol.* **289,** 371–384